

Fine structure of heavy excitons in GaAs/AlAs superlattices

C. Gourdon and P. Lavallard

*Groupe de Physique des Solides, Universités Paris 6 et Paris 7, Tour 23, 2 place Jussieu,
F75251 Paris CEDEX 05, France*

(Received 9 March 1992)

A splitting of the optically allowed states of the heavy exciton in GaAs/AlAs short-period, pseudo-direct superlattices was recently reported. Moreover, it was shown that the sublevels are dipole active along $\langle 110 \rangle$ crystallographic directions. In this work, the splitting energy, of the order of a few microelectronvolts, is determined for several samples from the period of the quantum beats observed in photoluminescence excited with a $\langle 100 \rangle$ polarized light. The time-resolved photoluminescence is analyzed within the framework of the density-matrix formalism to obtain the lifetime and spin-relaxation time of excitons. We show that the perturbation that splits the heavy-exciton states has the symmetry of either an electric field E_z along the growth axis or an ϵ_{xy} shear strain. This perturbation couples the heavy- and light-exciton states and gives a splitting energy proportional to the electron-hole exchange interaction and to the strength Z of the perturbation and inversely proportional to the energy difference between light and heavy excitons. The value of Z is found to be the same for all the samples studied, $Z = 14.5 \pm 1.5$ meV. We discuss possible origins of the perturbation.

I. INTRODUCTION

In the past few years, short-period GaAs/AlAs superlattices (SL) have been the subject of numerous studies in order to clarify the nature of the lowest electron confined state.¹⁻⁵ More recently, special attention has been paid to the fine structure of the lowest exciton state in short-period pseudodirect type-II SL's.⁶⁻⁹ In these SL's the lowest electron state arises from the X_z minimum of the conduction band in the AlAs layer (z is the $[001]$ growth axis). The optical transition that creates a heavy hole and an X_z electron is weakly allowed owing to the coupling of the X_z and Γ states by the SL potential. The photoluminescence (PL) spectrum shows a main luminescence line and phonon replica. The main line, which is Stokes shifted from the HH_1 - X_z maximum in the PL excitation spectrum, is attributed to the recombination of excitons localized by interface defects due to layer thickness fluctuations.

The lowest exciton state consists of four levels built from the heavy-hole states with projection of the total angular momentum along the growth axis $J_z = \pm \frac{3}{2}$ and the X_z electron states with spin $S_z = \pm \frac{1}{2}$. According to the SL crystallographic point group D_{2d} , two of them, which are optically allowed, belong to the two-dimensional Γ_5 representation (in Koster's notation¹⁰). The other two belong to the Γ_1 and Γ_2 representations and are optically forbidden. The allowed states are separated from the forbidden ones by the electron-hole exchange interaction. Surprisingly, a splitting of the allowed Γ_5 states was recently reported. This result was independently obtained, on the one hand, from the study of the polarization properties of luminescence⁶ and, on the other hand, from optically detected magnetic resonance (ODMR) by van Kesteren *et al.*⁷ Let us recall the main features of the PL degree of polarization of pseudodirect type-II SL's. Un-

der selective excitation of the localized exciton states with linearly polarized light, the main PL line and the phonon replica are strongly polarized like the excitation. The degree of linear polarization (DLP) is very anisotropic and depends on the angle between the direction of incident polarization and the $\langle 110 \rangle$ axes. The DLP can be as high as 80% for polarization along a $\langle 110 \rangle$ axis and is close to zero for polarization along a $\langle 100 \rangle$ axis. Under excitation with circularly polarized light, the degree of circular polarization (DCP) is also close to zero. These results, as well as those of van Kesteren *et al.*, led to the conclusion that the electric dipoles of the two excitonic sublevels (hereafter called X and Y) are aligned along the $\langle 110 \rangle$ crystallographic directions. The splitting energy is very small, of the order of a few μeV . So far its determination has been obtained (i) from ODMR spectra at zero magnetic field,⁷ (ii) from the decay of the DLP in a longitudinal magnetic field,⁸ and finally, (iii) as it was reported by van der Poel, Severens, and Foxon,⁹ from the observation of quantum beats between the two sublevels during PL time decay.

In this paper we report on the study of polarization quantum beats in several type-II samples, using various configurations of polarization. The experimental setup and the samples are described in Sec. II. In Sec. III, the experimental results are presented and analyzed within the framework of the density-matrix formalism. We obtain the exciton lifetime and spin-relaxation time as well as information about the existence and respective weight of two classes of excitons with opposite ordering of the X and Y sublevels. The transition from pseudodirect type-II to type-I SL's is investigated using a sample with a gradient of composition. We also report on results in a type-I sample. In Sec. IV, we consider the effect of perturbations of different symmetries on SL exciton states. We show that the perturbation that accounts for our results has the symmetry of an electric field E_z or a shear

strain ϵ_{xy} . The splitting energy is calculated. In Sec. V we determine the value of the ϵ_{xy} strain from the experimental splitting energies for samples of different compositions and we discuss the physical origin of the perturbation. A summary of the results is given in Sec. VI.

II. EXPERIMENTAL SETUP AND SAMPLE CHARACTERISTICS

All the results were obtained at pumped liquid-helium temperature. A dye laser synchronously pumped by an argon laser was used as the excitation source either in the cw or in the mode-locked regime. Selective excitation of localized excitonic states was used throughout this study. The cw or time-integrated DLP and DCP were measured with the use of a photoelastic modulator placed on the excitation beam. Time-resolved photoluminescence (TRL) was excited with pulses of width 10–20 ps. It was detected with a synchroscan streak camera with a time resolution of ≈ 30 ps. The time-resolved linear (circular) degree of polarization was measured with a polarizer (polarizer plus Fresnel rhomb) placed on the excitation beam and a fixed analyzer (quarter-wave plate plus analyzer). The linear and circular degrees of polarization are defined as usual as

$$\rho_{\text{lin}} = (I_{\parallel} - I_{\perp}) / (I_{\parallel} + I_{\perp})$$

for a linearly polarized excitation, and

$$\rho_{\text{circ}} = (I_{\sigma+} - I_{\sigma-}) / (I_{\sigma+} + I_{\sigma-})$$

for a circular σ_+ excitation.

Four GaAs/AlAs SL's, grown by molecular-beam epitaxy, were examined in this work. Their period and their mean concentration in Al were checked by x rays. Two of them, sample No. 1 (GaAs 18 Å/AlAs 12 Å) and sample No. 2 (GaAs 17 Å/AlAs 11 Å) are pseudodirect SL's close to the type-II–type-I transition. One of the samples, sample No. 3 (GaAs 20 Å/AlAs 8.7 Å) is a type-I SL. For sample No. 4 the rotation of the substrate holder was stopped during the growth to produce a spatial gradient of composition in the layer plane. The SL composition varies from (20.8 Å)/(12.2 Å) to (22.8 Å)/(11.2 Å) over a length $d_m = 23.4$ mm. The change in PL spectra recorded for several excitation spots between $x=0$ and $x=d_m$ is clear evidence of a smooth transition from pseudodirect type-II to type-I SL. One observes a progressive disappearance of phonon replica, an increase of the zero-phonon line intensity, and a shortening of PL decay time along the x direction. In all the samples the linewidth of the main PL line ranges from 6 to 10 meV.

Owing to experimental conditions, our study is restricted to SL's close to the type-II–type-I transition. In this region, a satisfactory PL signal-to-noise ratio can be achieved with resonant excitation and the decay time is not too long compared with the 12-ns period of the laser pulses.

III. EXPERIMENTAL RESULTS AND ANALYSIS

A. Splitting, lifetime, and spin-relaxation time

The study of the time behavior of the PL degree of polarization brings direct information about the splitting energy and the relaxation times. Since the splitting of the X and Y excitonic sublevels is much smaller than kT even at helium temperature, and also much smaller than the laser spectral width, the two sublevels can be coherently excited at time $t=0$ by a short pulse polarized along one of the $\langle 100 \rangle$ axes. As a consequence, the TRL signal, detected with polarization either parallel or perpendicular to the excitation, decays and oscillates with a period T inversely proportional to the splitting ΔE between the two sublevels ($T = \hbar / \Delta E$). The time behavior of the DLP $\rho_{\langle 100 \rangle}$ is shown in Fig. 1 for a type-II region of the graded sample. The period T is about 640 ps, which corresponds to a splitting energy of $\approx 6.3 \mu\text{eV}$. In samples No. 1 and No. 2, the splitting energies are found equal to 8.3 ± 0.5 and $9.3 \pm 0.5 \mu\text{eV}$, respectively. Let us recall that van Kesteren and van der Poel studied samples with different compositions and obtained splitting values in the same range although smaller (0.3, 0.7, and $1.5 \mu\text{eV}$).^{7,9}

The value of the splitting does not change with the detuning of the observation photon energy from the excitation energy (in the range 1–6 meV). Similarly, it hardly changes when the laser photon energy is scanned over 6 meV inside the PL line while keeping a fixed detuning. This means that the splitting almost does not depend on the localization energy of excitons.

Ivchenko *et al.* calculated the stationary degrees of polarization for various configurations of polarization

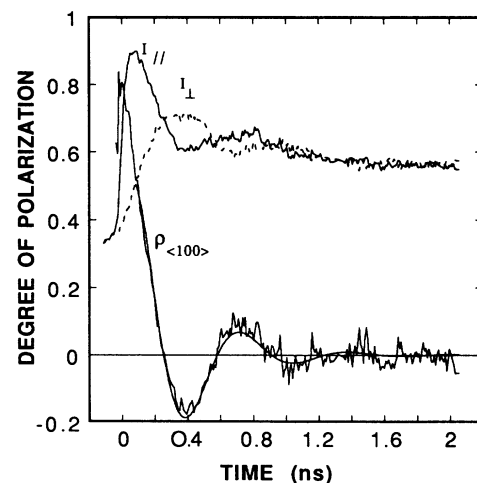


FIG. 1. Degree of polarization $\rho_{\langle 100 \rangle}$ for the composition-graded sample No. 4 in a type-II region close to the type-I–type-II transition [$x = 15.7$ mm, composition $\approx (22 \text{ \AA}) / (11.5 \text{ \AA})$]. The exciting beam is linearly polarized along a $\langle 100 \rangle$ axis. PL intensities I_{\parallel} and I_{\perp} are detected with polarization parallel and perpendicular to the excitation, respectively. $\rho_{\langle 100 \rangle}$ is fitted with $[\rho(0)\exp(-\delta t)\cos(\omega t)]$, where $\hbar\omega = 6.3 \mu\text{eV}$, $\hbar\delta = 2 \mu\text{eV}$, and $\rho(0) = 0.5$. The time origin is taken at the maximum of the I_{\parallel} signal.

within the framework of the density-matrix formalism.⁸ Along the same lines, we calculate the time dependence of the degrees of polarization after an excitation pulse. The density matrix ρ is written on the basis of the four excitonic states $|\pm\frac{1}{2}, \pm\frac{3}{2}\rangle$. The time evolution of ρ is given by

$$\frac{d\rho}{dt} = \frac{\partial\rho}{\partial t} - \frac{i}{\hbar}[H, \rho],$$

where $\partial\rho/\partial t$ describes the exciton recombination and spin relaxation and is written as in Ref. 8. The characteristic times of the excitonic system are the lifetime τ_0 and the total spin-relaxation time τ_s with

$$\tau_s^{-1} = (\tau_s^e)^{-1} + (\tau_s^h)^{-1}.$$

τ_s^e and τ_s^h are the electron and hole spin-relaxation times, respectively. The transverse and longitudinal relaxation times T and T' are related to τ_0 and τ_s by

$$T^{-1} = \tau_0^{-1} + \tau_s^{-1}$$

and

$$T'^{-1} = \tau_0^{-1} + (2\tau_s)^{-1}.$$

The observed splitting of the allowed states is taken into account in the Hamiltonian by introducing a nondiagonal matrix element

$$\langle \downarrow, \frac{3}{2} | H | \uparrow, -\frac{3}{2} \rangle = i \frac{\Delta E}{2} = i \frac{\hbar\omega}{2}.$$

This will be justified in Sec. IV. The initial excitation conditions are determined by the polarization of the exciting light pulse and by the optical selection rules. The results are summarized in Table I. They are obtained under the assumption that

$$\frac{T'^2}{4} [(\tau_s^e)^{-1} + (\tau_s^h)^{-1}]^2 (1 + TT'\Omega^2)^{-1} \ll 1,$$

where $\hbar\Omega$ is the splitting between the two optically forbidden states. With the values for T and T' obtained from experimental results, this inequality is fully verified.

One can notice that $\rho_{\langle 110 \rangle}(t)$ depends only on τ_s . On the other hand, the difference of the intensities $[I_{\langle 110 \rangle}(t) - I_{\langle 1\bar{1}0 \rangle}(t)]$ depends only on T and is propor-

tional to $\exp[-(t/T)]$. Although the PL decay time is longer than the 12-ns pulse period of our laser, we can measure the two parameters τ_s and T for composition-graded sample No. 4 close to the transition region [composition $\approx (22 \text{ \AA})/(11.5 \text{ \AA})$]. We find $\tau_s \approx 32$ ns, $T \approx 14$ ns, and then $\tau_0 \approx 28$ ns. These values are consistent with the cw DLP $\rho_{\langle 110 \rangle} = T'/\tau_0$ equal to 0.7. From the values of ω and τ_s one finds the parameter R in Table I nearly equal to 1, yielding

$$\rho_{\langle 100 \rangle}(t) \approx \frac{\exp[-t/(4\tau_s)]}{\cosh[t/(2\tau_s)]} \cos(\omega t).$$

Since the experimental value of τ_s is in the nanosecond range, the fast damping of the oscillations of $\rho_{\langle 100 \rangle}$ shown in Fig. 1 cannot only originate from spin relaxation and has to be attributed to the distribution of the splitting values around the mean value. We use a Lorentzian distribution of ω values of full width at half maximum 2δ to average the quantum beats in the PL signals I_{\parallel} and I_{\perp} . As a result, the theoretical DLP has to be multiplied by an additional damping term $[\exp(-\delta t)]$. Although this averaging method is not fully justified if δ is not much smaller than the mean value $\langle \omega \rangle$ of ω , $\rho_{\langle 100 \rangle}(t)$ was fitted in Fig. 1 using the expression

$$[\rho(0)\exp(-\delta t)\cos(\omega t)].$$

We find a rather large distribution of ω values with $\hbar\delta = 2$ μeV for $\hbar\omega = 6.3$ μeV . Similar results are obtained with the other type-II SL's.

However, let us note some discrepancy between the experimental cw degrees of polarization $\rho_{\langle 100 \rangle}$ and ρ_{σ} and the ones calculated with the above values for τ_0 , τ_s , and ω . Within the approximation discussed above, one has

$$\rho_{\langle 100 \rangle} = \frac{T'}{\tau_0} \frac{1}{1 + TT'\omega^2}$$

and

$$\rho_{\sigma} = \frac{T'^2}{\tau_0 T} \frac{1}{1 + TT'\omega^2},$$

which gives $\rho_{\langle 100 \rangle} \approx 2.4 \times 10^{-5}$ and $\rho_{\sigma} \approx 3 \times 10^{-5}$ for $\langle \omega \rangle$. Since $\rho_{\langle 100 \rangle}$ and ρ_{σ} decrease with ω , the smallest values of ω in the distribution contribute by a larger

TABLE I. Time-dependent degrees of polarization for heavy-exciton photoluminescence calculated within the framework of the density-matrix formalism (see text). The first line indicates the polarization of the exciting beam, i.e., linear polarization along a $\langle 110 \rangle$ or $\langle 100 \rangle$ axis or circular polarization. The first column indicates how the degree of polarization (DP) is measured: either with linear polarization along $\langle 110 \rangle$ or $\langle 100 \rangle$ axes or with circular polarization. The parameter R is equal to $[1 - (4\omega\tau_s)^{-2}]^{1/2}$.

Excitation	[110]	[100]	σ_+
DP			
$\rho_{\text{lin}\langle 110 \rangle}$	$\frac{2}{1 + \exp(t/\tau_s)}$		
$\rho_{\text{lin}\langle 100 \rangle}$		$\frac{\exp-t/(4\tau_s)}{\cosh[t/(2\tau_s)]} \left[\cos(R\omega t) - \frac{1}{4R\omega\tau_s} \sin(R\omega t) \right]$	$\frac{\exp-t/(4\tau_s)}{\cosh[t/(2\tau_s)]} \frac{\sin(R\omega t)}{R}$
ρ_{circ}		$\frac{\exp-t/(4\tau_s)}{\cosh[t/(2\tau_s)]} \frac{\sin(R\omega t)}{R}$	$\frac{\exp-t/(4\tau_s)}{\cosh[t/(2\tau_s)]} \left[\cos(R\omega t) + \frac{1}{4R\omega\tau_s} \sin(R\omega t) \right]$

weight to the degree of polarization. $\rho_{\langle 100 \rangle}$ averaged over the distribution of ω , with a width equal to $\langle \omega \rangle / 3$, is 27 times larger than $\rho_{\langle 100 \rangle}$ calculated for $\langle \omega \rangle$. However this is still smaller than the experimental values of $\rho_{\langle 100 \rangle}$ and ρ_{σ} found equal to $2.5 \pm 1\%$ and $1.5 \pm 1\%$, respectively. We attribute this discrepancy to the following. To fit the experimental PL decay curves and degrees of polarization, the time origin is taken at the maximum of the PL intensity, about 150 ps after the excitation pulse. During the risetime of PL, which is due to exciton relaxation among localized states, there is a small contribution to the degree of polarization. This is not taken into account in the analysis of the time-resolved PL.

B. Two classes of excitons

When the excitation light is σ_+ polarized and PL light is detected with linear polarization along $\langle 100 \rangle$ axes, the degree of polarization $\rho_{\langle 100 \rangle}^{\sigma}$ explicitly depends on the sign of $\Delta E = E_Y - E_X$ (cf. Table I). For two classes of excitons, with populations n_+ for $\Delta E > 0$ and n_- for $\Delta E < 0$,

$$\rho_{\langle 100 \rangle}^{\sigma} = \eta \frac{\exp[-t/(4\tau_s)] \sin(R\omega t)}{\cosh[t/(2\tau_s)] R},$$

with $\eta = (n_+ - n_-)/(n_+ + n_-)$. Only in the case of two classes of excitons with equal populations would the quantum beats be absent in $\rho_{\langle 100 \rangle}^{\sigma}$ (or $\rho_{\sigma}^{\langle 100 \rangle}$). We actually observe quantum beats in $\rho_{\langle 100 \rangle}^{\sigma}$. In sample No. 1, the amplitude of the oscillations for $\rho_{\langle 100 \rangle}^{\sigma}$ is smaller than for $\rho_{\langle 100 \rangle}$. Taking the inhomogeneous damping into account, we find $\eta = 0.66$ which gives $n_+/n_- \approx 5$. Van der Poel also observed that one class of excitons is strongly dominant over the other.⁹

C. From type-II to type-I superlattices

In the composition-graded sample No. 4, the splitting could be measured in the type-II region and in the transition region between type-II and type-I SL ($13 < x < 20$ mm). From type-II to type-I SL, while the PL decay time strongly decreases from ≈ 20 ns to ≈ 300 ps, the quantum beats amplitude decreases but the splitting remains rather constant. Very likely even in the type-I side of the transition region, the oscillations are due to localized $\text{HH}_1\text{-X}_z$ states that contribute to the long-time decay of the nonexponentially decreasing PL signal. Calculation shows that such states indeed exist at the same energy as $\text{HH}_1\text{-}\Gamma$ localized states.

Further into the type-I region, no oscillations of $\rho_{\langle 100 \rangle}$ are observed, but the cw DLP's $\rho_{\langle 110 \rangle}$ and $\rho_{\langle 100 \rangle}$, although approaching a common value, are still different (Fig. 2). Furthermore, the DCP remains very weak. Similar results are found in type-I sample No. 3: $\rho_{\langle 110 \rangle} = 0.26$, $\rho_{\langle 100 \rangle} = 0.11$, and $\rho_{\sigma} = 0.05$. This seems to indicate the existence of a splitting in short-period type-I SL's. However, it is difficult to determine its value, since no quantum beats are observed. Neither can it be determined from the cw degrees of polarization, since the small DCP is not consistent with the DLP's within the

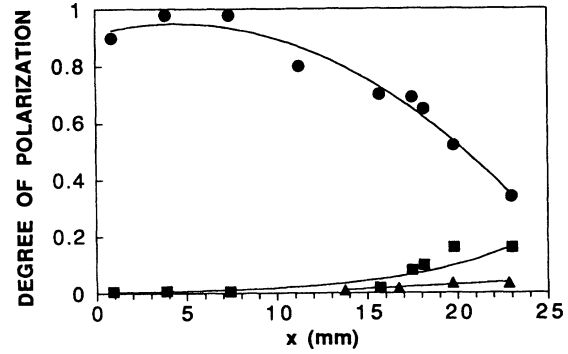


FIG. 2. cw DLP's $\rho_{\langle 110 \rangle}$ (circles) and $\rho_{\langle 100 \rangle}$ (squares) and DCP (triangles) are plotted as a function of the position of the exciting laser spot on the surface of the composition-graded sample No. 4. The solid lines are a guide for the eye. The smallest x values correspond to type-II SL and the largest to type-I SL. The transition region between type II and I determined from PL spectra is roughly located between $x = 13$ and $x = 20$ mm.

above model. As a matter of fact, most of the decay of the degree of polarization occurs during the rise time of luminescence. Despite the quasisonant excitation, the observed degree of polarization is related as much to the initially populated localized exciton states and the intermediate states as to the emitting states. The analysis of TRL in type-I samples is all the more difficult since one must use low excitation intensities because the time-integrated as well as time-resolved degrees of polarization are very much dependent on the excitation pulse intensity. For instance, in the composition-graded sample No. 4 ($x = 19.8$ mm, type-I side) we observe a decrease of the time-integrated DLP $\rho_{\langle 110 \rangle}$ from 52% to 22% when the light mean intensity increases from 0.4 W cm^{-2} to 400 W cm^{-2} . Since the absorption coefficient is larger, the initial density of excitons in type-I SL's is higher than in type-II SL's for the same sample thickness and the same light intensity. Exciton-exciton or exciton-carrier interaction contributes to a decrease of the spin relaxation time and hence to a decrease of the degree of polarization.

IV. PERTURBATION HAMILTONIAN

Since in pseudodirect type-II SL's the optical transition is allowed at $k=0$, we will only consider hereafter excitons built up from Γ electron and Γ hole states. From group theory, it is found that only a perturbation Hamiltonian belonging to the one-dimensional Γ_2 , Γ_3 , or Γ_4 representations of D_{2d} can split the Γ_5 exciton level. A Γ_2 element transforms like the z component of an axial vector as, for instance, a magnetic field and will not be considered hereafter. A Γ_3 element transforms like $(x^2 - y^2)$ as, for example, an $(\epsilon_{xx} - \epsilon_{yy})$ strain caused by a uniaxial stress along a $\langle 100 \rangle$ axis. A Γ_4 element transforms like z as an electric field E_z or like xy as an ϵ_{xy} strain.

The situation encountered in GaAs/AlAs superlattices is very similar to the case of wurtzite semiconductors

with C_{6v} symmetry (like CdS and CdSe) subjected to a uniaxial stress perpendicular to the hexagonal axis. It has been known for a long time that in these conditions, both the A and B exciton states (which are very similar to the heavy and light excitons) split linearly with the applied stress, although the valence and conduction bands do not split.¹¹ This effect was understood in terms of an interplay between applied stress and exchange interaction. Let us note that for C_{6v} , (x^2-y^2) and xy belong to the same representation and z belongs to a different one, whereas in the D_{2d} (or in T_d) group, xy and z belong to the same representation and (x^2-y^2) to a different one. To investigate the effect of Γ_3 and Γ_4 perturbations, we use the comprehensive work of Cho, who studied the effect of all possible symmetry-breaking perturbations on cubic semiconductors within a group-theoretical approach.¹²

The crystallographic point group of GaAs/AlAs SL's is the same as the one of cubic semiconductors under uniaxial pressure. Therefore, we start from the excitonic states of a cubic semiconductor and first apply a perturbation with the symmetry of a stress along [001]. The Hamiltonian of Table 2.3 of Ref. 12 is diagonalized to obtain the heavy (HE) and light (LE) exciton states of a superlattice. Each of them consists of four states, two of them optically allowed and two of them optically forbidden. Here, we neglect any coupling with the exciton-states split off by the spin-orbit interaction. In electron-hole notation, the allowed HE and LE states are written

$$|\text{HE}_1\rangle = \frac{-i}{\sqrt{2}} [|\uparrow, -\frac{3}{2}\rangle + |\downarrow, \frac{3}{2}\rangle]$$

$$|\text{HE}_2\rangle = \frac{1}{\sqrt{2}} [|\uparrow, -\frac{3}{2}\rangle - |\downarrow, \frac{3}{2}\rangle],$$

and

$$|\text{LE}_1\rangle = \frac{i}{\sqrt{2}} [|\downarrow, -\frac{1}{2}\rangle + |\uparrow, \frac{1}{2}\rangle],$$

$$|\text{LE}_2\rangle = \frac{1}{\sqrt{2}} [|\downarrow, -\frac{1}{2}\rangle - |\uparrow, \frac{1}{2}\rangle].$$

We take into account the electron-hole exchange interaction, which is of prime importance, as we shall see later. The exchange Hamiltonian is written as

$$H_{\text{exc}} = a_0 - a \sum_{i=x,y,z} J_{h,i} S_{e,i} - b \sum_{i=x,y,z} J_{h,i}^3 S_{e,i},$$

with $a_0 = 3a/4$. $J_{h,i}$ and $S_{e,i}$ are the components of the hole total angular momentum \mathbf{J}_h and the electron spin \mathbf{S}_e , respectively. The quantization axis is the SL growth axis. We use the same Hamiltonian as van Kesteren *et al.*⁷ but we do not drop the diagonal term a_0 . The parameter a is equal to $2(j_0 - j_1)$ in the notations of Cho. The exchange energy E , defined as the separation between the allowed HE states and the center of gravity of the HE forbidden states, is equal to $\frac{3}{2}[a + (9b/4)]$. The splitting $\hbar\Omega$ between the forbidden Γ_1 and Γ_2 HE states is equal to $3b/2$.

Let us first consider the effect of a z (or xy) perturba-

tion. The Hamiltonian in the basis of HE and LE states has the following expression:

$$H = \begin{pmatrix} |\text{HE}_1\rangle & |\text{HE}_2\rangle & |\text{LE}_1\rangle & |\text{LE}_2\rangle \\ 0 & 0 & E' & -Z \\ & 0 & Z & -E' \\ & & \Delta_{lh} & 0 \\ & & & \Delta_{lh} \end{pmatrix},$$

where only the upper right half of the matrix is written. The origin of energies is taken for the HE states. Δ_{lh} is the energy difference between the LE and HE states. E' is related to the parameters of the exchange Hamiltonian by $E' = (\sqrt{3}/2)[a + (7b/4)]$ and Z is the matrix element of a perturbation of symmetry z or xy ($Z = 2Z_1$ in the notations of Ref. 12). Using a perturbation treatment, one finds the following eigenenergies:

$$E'_{h\pm} = -\frac{(E' \pm Z)^2}{\Delta_{lh}}$$

and

$$E'_{l\pm} = \Delta_{lh} + \frac{(E' \pm Z)^2}{\Delta_{lh}}.$$

The splitting of HE (and LE) allowed exciton states is equal to $(4E'Z/\Delta_{lh})$. It is worth noting that neither the exchange interaction alone nor a Z perturbation alone can split the exciton states. In the case of an ε_{xy} strain component, Z is simply equal to $d\varepsilon_{xy}$, where d is the deformation potential for a stress along [111] direction.

The split states are now $|\text{HE}_X\rangle$ and $|\text{HE}_Y\rangle$, with

$$|\text{HE}_X\rangle = \frac{1}{\sqrt{2}} [|\text{HE}_1\rangle - |\text{HE}_2\rangle]$$

and

$$|\text{HE}_Y\rangle = \frac{1}{\sqrt{2}} [|\text{HE}_1\rangle + |\text{HE}_2\rangle].$$

$|\text{HE}_X\rangle$ and $|\text{HE}_Y\rangle$ are indeed dipole active for [110] and $[1\bar{1}0]$ polarizations, respectively, which agrees well with our experimental findings. We now return to the expression of the Hamiltonian used in the density-matrix treatment. It is easily found that the perturbation that mixes HE and LE states can be simply expressed as an off-diagonal term of the Hamiltonian in the subspace of allowed and forbidden HE states with

$$\langle \downarrow, \frac{3}{2} | H | \uparrow, -\frac{3}{2} \rangle = i \frac{\Delta E}{2},$$

with

$$\Delta E = \frac{4E'Z}{\Delta_{lh}}.$$

The same calculation was carried out for a stress applied along the [100] or [010] axis. With the notations of Cho, this stress gives rise to two perturbation matrix elements $U = \sqrt{3}(\varepsilon_{xx} - \varepsilon_{yy})$ and $V = 2\varepsilon_{zz} - \varepsilon_{xx} - \varepsilon_{yy}$, where

$U = -\sqrt{3}V$. Again, one finds a splitting proportional to $E'U/\Delta_{lh}$, but the eigenstates are dipole active along the [100] and [010] axes. Therefore, this perturbation is not relevant to our case.

V. DISCUSSION

In order to compare the theoretical splitting for a Z perturbation with our experimental values, we need to evaluate the matrix element $E' = (\sqrt{3}/2)[a + (7b/4)]$ of the perturbation Hamiltonian. This term is nearly equal to the exchange energy E divided by $\sqrt{3}$ if b is much smaller than $2a$. We assume that this inequality is verified for our samples as it is for van Kesteren *et al.*⁷ In our samples, the exchange energy is not known but can be estimated from the exchange energy in samples of van Kesteren *et al.*, assuming that it is proportional to $|\langle X_z | HH_1 \rangle|^2$, the overlap of electron and hole envelope wave functions.¹³ In Fig. 3, the splitting ΔE between the HE-allowed states is plotted as a function of $|\langle X_z | HH_1 \rangle|^2/\Delta_{lh}$. The squares represent the results of van Kesteren *et al.*⁷ and van der Poel, Severens, and Foxon,⁹ and the dots represent our results. The linear behavior suggests that the perturbation has a constant amplitude, $Z = 14.5 \pm 1.5$ meV.

In D_{2d} symmetry, this perturbation may originate from an ε_{xy} shear strain or from an electric field E_z through piezoelectric interaction. From $Z = d\varepsilon_{xy}$, using the deformation potential d of GaAs ($d = -4.55$ eV),¹⁴ we find $\varepsilon_{xy} = 3.2 \pm 0.3 \times 10^{-3}$. The relation between stress (σ_{ij} tensor), strain, and electric field is given in D_{2d} symmetry by the piezoelectric equation

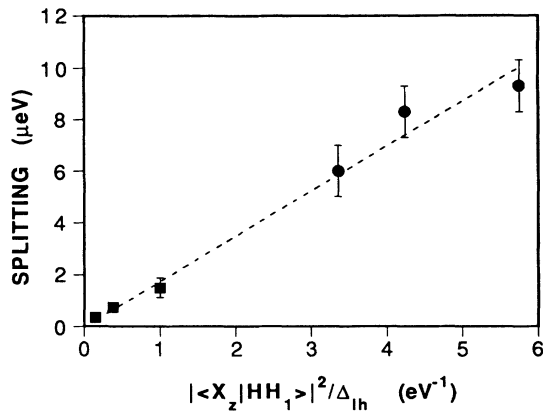


FIG. 3. The excitonic splitting for various GaAs/AlAs SL samples is plotted as a function of the overlap of HH_1 and X_z envelope functions divided by the difference of confinement energies for heavy and light holes. The samples of van Kesteren *et al.* (see Table I of Ref. 7) are represented by squares and ours by dots. From left to right the sample composition is [(23 Å)/(41 Å)], [(23 Å)/(28 Å)], [(22 Å)/(19 Å)], [(22 Å)/(12 Å)], [(18 Å)/(12 Å)], [(17 Å)/(11 Å)].

$$\sigma_{xy} = 2c_{66}\varepsilon_{xy} - e_{36}E_z,$$

where the elastic stiffness coefficient c_{66} and the piezoelectric stress constant e_{36} are written in Voigt notation. It is very improbable that all the samples are subjected to an external σ_{xy} shear stress; hence, we take $\sigma_{xy} = 0$. Using the values of c_{66} and e_{36} known for GaAs ($c_{66} = c_{44} = 5.9 \times 10^{10}$ N m⁻² and $e_{36} = e_{14} = -0.16$ C m⁻²),¹⁴ we find $E_z = 24\,000$ kV cm⁻¹. This is much larger than any reasonable value for an electric field in a SL. Therefore, the effect of an internal electric field in the SL is negligible and will not be considered anymore.

In type-II SL's, as a result of the confinement of electrons and holes in adjacent layers, the maxima of the exciton envelope function are located at the interfaces. Moreover, in the case of a localized exciton, the wave function does not extend coherently over many periods of the SL but very likely peaks at one particular interface. There, the [110] and $[1\bar{1}0]$ directions are not equivalent and the symmetry is lower than D_{2d} . Assuming that the relation between stress and strain tensor components are still valid in a small volume of a few lattice cells, and taking into account the fact that the symmetry is only C_{2v} at the interface, one finds

$$\sigma_{xy} = 2c_{66}\varepsilon_{xy} + \alpha(\varepsilon_{xx} + \varepsilon_{yy}) + \beta\varepsilon_{zz}.$$

The subscripts x and y still refer to the [100] and [010] axes. The parameters α and β , which are equal to zero in D_{2d} symmetry, are proportional to the difference of two elastic stiffness coefficients in C_{2v} symmetry. They are at most of the same order of magnitude as the stiffness coefficients. From the four elastic equations relating σ_{xx} , σ_{yy} , σ_{zz} , and σ_{xy} and the strain tensor components ε_{xx} , ε_{yy} , ε_{zz} , and ε_{xy} , the latter can be determined by setting as external conditions $\sigma_{xx} \neq 0$, $\sigma_{yy} \neq 0$, $\sigma_{xx} = \sigma_{yy}$, $\sigma_{zz} = 0$, and $\sigma_{xy} = 0$. This takes into account the fact that the AlAs layers are under biaxial compression because the lattice parameter is imposed by the GaAs substrate. Unfortunately, α and β are unknown parameters. However, it seems possible to obtain a shear strain ε_{xy} of the same order of magnitude as the strain caused by the GaAs/AlAs lattice mismatch. To summarize, owing to the fact that AlAs layers are under biaxial compression, a shear strain may appear at the interface, i.e., a difference ($\varepsilon_{xx} - \varepsilon_{yy}$) between strains in [110] and $[1\bar{1}0]$ directions.

In order to explain the existence of a mean value of the splitting energy, one has to assume that within the in-plane extension of the exciton wave function, interface roughness is characterized by the existence of few defects with very small dimensions. On the other hand, these defects, as well as the spatial extension of the exciton envelope function over the adjacent interfaces in the z direction, account for the broad distribution of ΔE values around the mean value. Depending on the parity of the number of GaAs and AlAs monolayers in each layer, there exists either one or two kinds of interface: one with Al-As bonds lying in the (110) plane and the other with Al-As bonds in the $(1\bar{1}0)$ plane. The two classes of excitons might be related to these two kinds of interface. The

fact that one class of excitons has a larger population than the other would indicate that one kind of interface exhibits smaller scale roughness or has incorporated more impurities than the other. It is worthwhile noting that it is only in the case of a $[\text{GaAs}(2n)]/[\text{AlAs}(2n)]$ SL that the two kinds of interfaces can be identified with the GaAs/AlAs and AlAs/GaAs interfaces, which are known to be of different qualities.¹⁵ Unfortunately, the composition of the investigated SL's most often does not correspond to integer numbers of monolayers, so that it is not possible to relate the two classes of excitons to GaAs/AlAs and AlAs/GaAs interfaces.

In short-period type-I SL's, it seems more difficult to explain the existence of a splitting, since the envelope function of a localized exciton has its maximum at the center of one GaAs layer and extends over the neighboring AlAs/GaAs and GaAs/AlAs interfaces. Only if one of these interfaces has a much smaller scale disorder than the other, or in the case of a $[\text{GaAs}(2n+1)]/[\text{AlAs}(2n+1)]$ SL for which the two interfaces are similar, can the existence of a splitting be understood.

VI. SUMMARY

From the quantum beats observed in the decay of photoluminescence excited with a $\langle 100 \rangle$ polarized pulse, we determined the splitting of the optically allowed heavy-exciton states for several type-II GaAs/AlAs superlattices. The analysis of the decay of the polarized photoluminescence, using the results of density-matrix calculation, gives the exciton lifetime and spin-relaxation time, which are both in the range of several tens of ns for type-II samples.

We showed that the splitting is nearly equal to

$4EZ/\sqrt{3}\Delta_{lh}$, where E is the electron-hole exchange energy, Δ_{lh} the light- and heavy-exciton energy separation, and Z the strength of the perturbation, which has the same symmetry as an electric field E_z or an ϵ_{xy} strain. The variation of the splitting with the SL composition gives a perturbation of constant amplitude $Z = 14.5$ meV, which corresponds to a shear strain $\epsilon_{xy} = 3.2 \times 10^{-3}$. The dissymmetry between $[110]$ and $[\bar{1}\bar{1}0]$ directions at the interface, together with the biaxial compression of AlAs layers, may qualitatively explain the existence of the splitting.

The anisotropy of the linear degree of polarization as well as a weak degree of circular polarization are also observed in type-I short-period superlattices and seem to indicate the existence of a splitting. However, no quantum beats can be observed, most probably because the spin-relaxation time is very short as compared to the lifetime. More work is needed to derive a definite conclusion regarding the existence and value of the splitting in type-I samples.

ACKNOWLEDGMENTS

We are grateful to Richard Panel from the Laboratory of Microstructures and Microelectronics for his collaboration in this work, including the growth of the samples and many scientific discussions. We also acknowledge very stimulating and fruitful discussions with E. L. Ivchenko from Ioffe Physico-Technical Institute (St. Petersburg, Russia). The Groupe de Physique des Solides is "Unité de recherche propre du Centre National de la Recherche Scientifique No. 17." The Laboratory of Microstructures and Microelectronics is "Unité de recherche propre du Centre National de la Recherche Scientifique No. 20."

¹D. Scalbert, J. Cernogora, C. Benoit à la Guillaume, M. Maaref, F. F. Charfi, and R. Panel, *Solid State Commun.* **70**, 945 (1989).
²H. W. van Kesteren, E. C. Cosman, P. Dawson, K. J. Moore, and C. T. Foxon, *Phys. Rev. B* **39**, 13 426 (1989).
³M. S. Skolnick, G. W. Smith, I. L. Spain, C. R. Whitehouse, D. C. Herbert, D. M. Whittaker, and L. J. Reed, *Phys. Rev. B* **39**, 11 191 (1989).
⁴P. Dawson, C. T. Foxon, and H. W. van Kesteren, *Semicond. Sci. Technol.* **5**, 54 (1990).
⁵E. Finkman, M. D. Sturge, M.-H. Meynadier, R. E. Nahory, M. C. Tamargo, D. H. Hwang, and C. C. Chang, *J. Lumin.* **39**, 57 (1987).
⁶S. Permogorov, A. Naumov, C. Gourdon, and P. Lavallard, *Solid State Commun.* **74**, 1057 (1990).
⁷H. W. van Kesteren, E. C. Cosman, W. A. J. A. van der Poel, and C. T. Foxon, *Phys. Rev. B* **41**, 5283 (1990).

⁸E. L. Ivchenko, V. P. Kochereshko, A. Yu. Naumov, I. N. Uraltsev, and P. Lavallard, *Superlatt. Microstruct.* **10**, 497 (1991).
⁹W. A. J. A. van der Poel, A. L. G. J. Severens, and C. T. Foxon, *Opt. Commun.* **76**, 116 (1990).
¹⁰G. F. Koster, J. O. Dimmock, R. G. Wheeler, and H. Statz, *Properties of the 32 Point Groups* (MIT, Cambridge, MA, 1963).
¹¹O. Akimoto and H. Hasegawa, *Phys. Rev. Lett.* **20**, 916 (1968).
¹²K. Cho, in *Excitons*, edited by K. Cho, Topics in Current Physics Vol. 14 (Springer-Verlag, Berlin, 1979), p. 16.
¹³B. Rejaei Salmassi and G. E. W. Bauer, *Phys. Rev. B* **39**, 1970 (1989).
¹⁴S. Adachi, *J. Appl. Phys.* **58**, R1 (1985).
¹⁵P. M. Petroff, R. C. Miller, A. C. Gossard, and W. Wiegmann, *Appl. Phys. Lett.* **44**, 217 (1984).